

THICKNESS-DEGRADATION-FREE DIELECTRIC THIN FILMS

The thin-film dielectric is one of the most important components of current electronic devices and the heart of these devices is the parallel plate capacitor where a thin film of dielectrics is sandwiched by a pair of electrodes. For the realization of high-density and high-performance devices, it is necessary to make higher-density capacitors by the utilization and scaling down of thin films of novel dielectric materials having a high relative dielectric constant above 200. Leading candidates for these materials are simple perovskite-structured oxides, schematically drawn in Fig. 1(a), as typified by SrTiO_3 and $(\text{Ba,Sr})\text{TiO}_3$ [1,2]. However, a marked drop of the dielectric constant with the decrease in film thickness, widely known as the “size effect,” is frequently reported to be serious especially for these high-dielectric-constant materials [1,2]. In this article, we propose thin films of *c*-axis-oriented bismuth layer-structured dielectrics (BLDs) as novel candidates for size-effect-free materials to overcome these problems (refer to the detail in [3]).

BLDs have a natural superlattice structure along the *c*-axis consisting of two kinds of 2-dimensional nanolayers, i.e., $(\text{Bi}_2\text{O}_2)^{2+}$ and a pseudoperovskite block generally described as $(\text{A}_{m-1}\text{B}_m\text{O}_{3m+1})^{2-}$, where *m* is the number of BO_6 octahedra in pseudoperovskite blocks as schematically shown in Figs. 1(b) and 1(c). BLDs with an even *m*-number show no ferroelectricity along the *c*-axis because of the mutual counterbalance of their polarity due to a mirror plane in the pseudoperovskite layer. Therefore, *c*-axis-oriented BLD films with an even *m*-number act as paraelectric.

c-axis-oriented epitaxial $\text{SrBi}_4\text{Ti}_4\text{O}_{15}$ and $\text{CaBi}_4\text{Ti}_4\text{O}_{15}$ films with various thicknesses were grown at 700 °C by metalorganic chemical vapor deposition (MOCVD). $(001)_c$ -oriented epitaxial SrRuO_3 films having an atomically flat surface grown on $(001)\text{SrTiO}_3$ single crystals by MOCVD

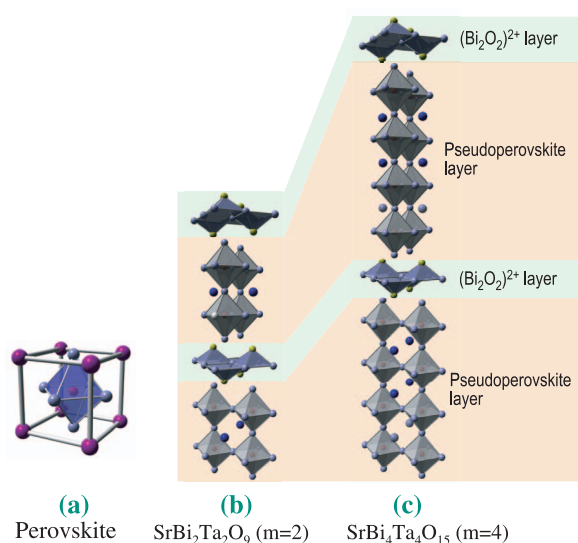


Fig. 1. Schematic diagrams of crystal structure. (a) simple perovskite structure, (b) $\text{SrBi}_2\text{Ta}_2\text{O}_9$ ($m=2$), and (c) $\text{SrBi}_4\text{Ti}_4\text{O}_{15}$ ($m=4$).

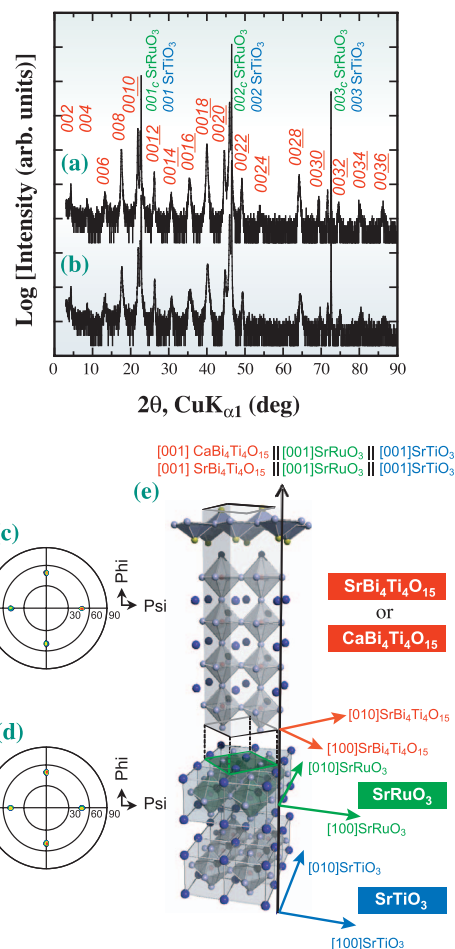


Fig. 2. ((a) and (b)) X-ray diffraction patterns and ((c) and (d)) X-ray pole figure measurement of *c*-axis-oriented epitaxial. ((a) and (c)) $\text{SrBi}_4\text{Ti}_4\text{O}_{15}$ and ((b) and (d)) $\text{CaBi}_4\text{Ti}_4\text{O}_{15}$ films grown on $(100)_c\text{SrRuO}_3$ / $(100)\text{SrTiO}_3$ substrates. The fixed 2θ angle corresponds to 119 diffractions of each phase. (e) Schematic diagrams indicating the epitaxial relationship between $\text{SrBi}_4\text{Ti}_4\text{O}_{15}$, SrRuO_3 and SrTiO_3 .

were used as substrates.

The constituent phase and orientation of the films were identified by conventional X-ray diffraction (XRD) analysis using a high-resolution four-circle diffractometer and $\text{Cu-K}\alpha_1$ radiation. The crystal structure was examined in detail by XRD analysis using synchrotron radiation at beamline BL13XU [4] with a wavelength of 0.99 Å.

Figure 2 shows the typical XRD patterns of 98 nm- and 85 nm-thick (a) $\text{SrBi}_4\text{Ti}_4\text{O}_{15}$ and (b) $\text{CaBi}_4\text{Ti}_4\text{O}_{15}$ films grown on $(001)_c\text{SrRuO}_3$ / $(001)\text{SrTiO}_3$ substrates, respectively. Only the $002l$ ($l = \text{integer number}$) peaks of each BLD phase were observed. Epitaxial growth of these films was confirmed by X-ray pole figure measurement as can be seen in Figs. 2(c) and 2(d), i.e., $(001)\text{SrBi}_4\text{Ti}_4\text{O}_{15}$ or $\text{CaBi}_4\text{Ti}_4\text{O}_{15}$ / $(001)_c\text{SrRuO}_3$ / $(001)\text{SrTiO}_3$ [see Fig. 2(e)].

Figure 3(a) shows the film thickness dependences of surface-normal and in-plane lattice parameters, and the unit

cell volume of epitaxial $\text{SrBi}_4\text{Ti}_4\text{O}_{15}$ films, where each value indicates the change normalized by those of the 154 nm-thick film. The in-plane lattice parameter gradually increased with film thickness scaling, indicating the increase in in-plane residual strain. Hence, the maximum misfit strain was induced when the in-plane lattice of $\text{SrBi}_4\text{Ti}_4\text{O}_{15}$ was fully clamped by that of the SrRuO_3 interlayer without any misfit dislocations, and then the misfit strain exponentially decreased, as seen in Fig. 3(a), with the increase in film thickness and the release of the clamping of the in-plane $\text{SrBi}_4\text{Ti}_4\text{O}_{15}$ lattice through the induction of the misfit dislocations. Here, the residual strain change between thinnest and thickest $\text{SrBi}_4\text{Ti}_4\text{O}_{15}$ films was 56%, which corresponds to a 10% decrease in dielectric constant according to a report on the mechanical bending of $(\text{Ba}_{0.7}\text{Sr}_{0.5})\text{TiO}_3$ films [5]. On the other hand, the surface-normal lattice parameter decreased with the increase in the in-plane one to maintain unit cell volume. However, surprisingly, unit cell volume increased with the decrease in film thickness as shown in Fig. 3(b). Figure 3(c) shows the room temperature relative dielectric constant as a function of the film thickness of *c*-axis-oriented epitaxial $\text{SrBi}_4\text{Ti}_4\text{O}_{15}$ and $\text{CaBi}_4\text{Ti}_4\text{O}_{15}$ films, where those of $\text{SrBi}_2\text{Ta}_2\text{O}_9$ films and the reported data for $(\text{Ba}_{0.5}\text{Sr}_{0.5})\text{TiO}_3$ films (dotted line) are also shown for comparison. $\text{SrBi}_4\text{Ti}_4\text{O}_{15}$ films did not show any degradation in dielectric constant with the decrease in film thickness down to 17 nm, corresponding to about 4 unit cells ($c = 4.040$ nm), indicating the size-effect-free dielectric characteristics. This result clearly indicates that in-plane stress applied to *c*-axis-oriented $\text{SrBi}_4\text{Ti}_4\text{O}_{15}$ films hardly affects their dielectric characteristics. Moreover, the relative dielectric constants of $\text{SrBi}_4\text{Ti}_4\text{O}_{15}$ and $\text{CaBi}_4\text{Ti}_4\text{O}_{15}$ films were almost 200 for both films irrespective of the type of cation in pseudoperovskite blocks. Furthermore, these values were around 4 times larger than that of $\text{SrBi}_2\text{Ta}_2\text{O}_9$ films with an *m*-number of 2, suggesting that the dielectric constant of BLDs was mainly determined by *m*-number.

The marked drop of dielectric constant with the decrease in film thickness as in $(\text{Ba}_{0.5}\text{Sr}_{0.5})\text{TiO}_3$ films shown in Fig. 3(c) is generally explained by the dead layer model. Figure 3(d) plots the thickness dependence of the reciprocal capacitance of $\text{SrBi}_4\text{Ti}_4\text{O}_{15}$ films, where data for $\text{SrBi}_2\text{Ta}_2\text{O}_9$ and $(\text{Ba}_{0.5}\text{Sr}_{0.5})\text{TiO}_3$ films (dotted line) are also shown for comparison. For $(\text{Ba}_{0.5}\text{Sr}_{0.5})\text{TiO}_3$ films, the thickness dependence of the reciprocal capacitance showing a linear relationship did not cross the zero point. This indicates that the data for these $(\text{Ba}_{0.5}\text{Sr}_{0.5})\text{TiO}_3$ films were followed by the dead layer model, suggesting the existence of the dead layer having a low dielectric constant between these $(\text{Ba}_{0.5}\text{Sr}_{0.5})\text{TiO}_3$ films and electrodes. On the other hand, data for $\text{SrBi}_4\text{Ti}_4\text{O}_{15}$ and $\text{SrBi}_2\text{Ta}_2\text{O}_9$ films cross the zero point as shown in Fig. 3(d), followed by the simple single capacitor model.

The results of the present study suggest that the film-thickness-independent dielectric characteristics are the common features for the BLD with even an *m*-number. This result indicates that a natural superlattice structure parallel to the direction of the applied electric field is the key for realizing size-effect-free characteristics and in-plane orientation does not affect it.

In summary, *c*-axis-oriented $\text{SrBi}_4\text{Ti}_4\text{O}_{15}$ and $\text{CaBi}_4\text{Ti}_4\text{O}_{15}$ films with various thicknesses were epitaxially grown on $(100)_c\text{SrRuO}_3// (100)\text{SrTiO}_3$ substrates by MOCVD. The relative dielectric constant of these films kept a constant value of 200 irrespective of the film thickness down to 17 nm, indicating size-effect-free dielectric characteristics. These dielectric characteristics were considered to be brought about the dielectric constant being extremely insensitive dielectric constant to the residual strain in the films induced by exogenetic stresses, such as thermal, misfit and electrostrictive ones. The dead-layer-free interface was also a critical factor especially for size-effect-free dielectric characteristics. These characteristics are very attractive for high-density capacitor applications.

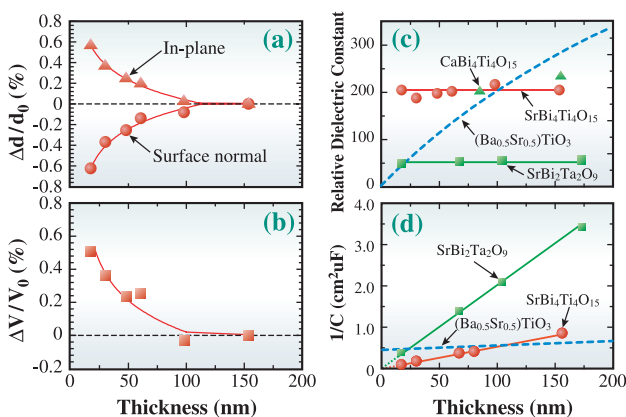


Fig. 3. Thickness dependences of (a) surface-normal and in-plane lattice parameters, and (b) unit cell volume of $\text{SrBi}_4\text{Ti}_4\text{O}_{15}$ films. Thickness dependences of (c) relative dielectric constants of $\text{SrBi}_4\text{Ti}_4\text{O}_{15}$ and $\text{CaBi}_4\text{Ti}_4\text{O}_{15}$ films together with those of $\text{SrBi}_2\text{Ta}_2\text{O}_9$ films. (d) Reciprocal capacitance as a function of thickness of $\text{SrBi}_4\text{Ti}_4\text{O}_{15}$ films.

Hiroshi Funakubo^{a,b,*} and Osami Sakata^c

^a Department of Innovative and Engineered Materials, Tokyo Institute of Technology

^b PRESTO, Japan Science and Technology Agency (JST)

^c SPring-8 / JASRI

*E-mail: funakubo.h.aa@m.titech.ac.jp

References

- [1] C.S. Hwang *et al.*: Jpn. J. Appl. Phys. **34** (1995) 5178.
- [2] L.J. Sinnamon *et al.*: Appl. Phys. Lett. **78** (2001) 1724.
- [3] K. Takahashi, M. Suzuki, T. Kojima, T. Watanabe, Y. Sakashita, K. Kato, O. Sakata, K. Sumitani and H. Funakubo: Appl. Phys. Lett. **89** (2006) 082901.
- [4] O. Sakata *et al.*: Surf. Rev. Lett. **10** (2003) 543.
- [5] T. Shaw *et al.*: Appl. Phys. Lett. **75** (1999) 2129.